

Dielectric properties of WS₂-coated multiwalled carbon nanotubes studied by energy-loss spectroscopic profiling

Vlad Stolojan and S. R. P. Silva^{a)}

Advanced Technology Institute, University of Surrey, Guildford, GU2 7XH, United Kingdom

Michael J. Goringe

School of Engineering, University of Surrey, Guildford, GU2 7XH, United Kingdom

R. L. D. Whitby, Wang K. Hsu, D. R. M. Walton, and Harold W. Kroto

School of Chemistry, Physics and Environmental Sciences, University of Sussex, Brighton, BN1 9QJ, United Kingdom

(Received 29 July 2004; accepted 7 December 2004; published online 3 February 2005)

We investigate experimentally the electronic properties of the coating for multiwalled carbon nanotubes covered in tungsten disulfide (WS₂) of various thicknesses. Coatings of thicknesses between 2 and 8 monolayers (ML) are analyzed using energy-loss spectroscopic profiling (ELSP), by studying the variations in the plasmon excitations across the coated nanotube, as a function of the coating thickness. We find a change in the ELSP for coatings above 5 ML thickness, which we interpret in terms of a change in its dielectric properties. © 2005 American Institute of Physics.

[DOI: 10.1063/1.1861985]

The discovery of carbon nanotubes¹ and fullerenes² has started a significant research effort into developing carbon electronics as a possible alternative to the end-of-the-road for silicon-based electronics, which is predicted to be reached in the next 10–15 years. Recent advances in controlling the growth of nanotubes³ and the manipulation and welding of individual nanotubes⁴ have brought the goal of producing working carbon devices within reach. Carbon nanotubes coated with functional layers are excellent candidates as starting blocks for these devices. The heterojunctions formed at multiwalled carbon nanotubes (MWCNTs) coated with WS₂, a known bulk semiconductor,⁵ could have applications in high-efficiency large-area photovoltaics and light-emitting structures. Their use, however, requires knowledge of the dielectric properties of the coating, as a function of its thickness, which we investigate here.

This information can be acquired in a general-purpose transmission electron microscope (TEM) fitted with a Gatan imaging filter (GIF) using a technique known as energy-loss spectroscopic profiling (ELSP),^{6,7} without the need for focusing the electron probe to subnanometer sizes. While the spatial sampling of the electronic structure information obtained in this manner is below that of a dedicated scanning TEM, it has significantly better spatial resolution than if the same TEM were used to form a small electron probe, whose diameter is not smaller than 1.5 nm in our case.⁸

MWCNTs coated with a varying number of ordered WS₂ layers were produced by pyrolysis; the production method and the characteristics of the nanotube and the coating are described elsewhere.⁵ The tungsten disulfide coating appears to cover the nanotubes along their whole length. Small coating thickness variations [1–2 monolayers (ML)] can occur along the length of the nanotube, so we only analyzed regions where the coating thickness was constant over lengths 5–10 times the nanotube's diameter. There was no detectable oxygen [using electron energy loss spectroscopy (EELS)] in

the coating. The samples were analyzed using a Philips CM200TEM with a LaB₆ filament, fitted with a GIF2000 spectrometer.

When orienting a linear feature along the axis integrated by the quadrupoles of the GIF, the CCD records a two-dimensional image where one coordinate is the energy loss and other is, to within a scaling factor, the spatial coordinate normal to the linear feature; this technique is ELSP.⁷ Here we use a tilt-rotate holder to accurately align the tube along the integrated axis to within 0.1°. The data are gathered in the diffraction-coupled mode (i.e., the image appears on the screen but the spectrometer is focused on the beam crossover where one records the diffraction pattern), using the largest collector aperture available (3 mm), at ~820 000× magnification. The choice of collection angle for samples with an anisotropic dielectric function can alter the relative contributions of each of the dielectric components, but as the experiments for all coating thicknesses were performed at the same camera length and with the same collector aperture, the influence of the collection angle is also the same for all thicknesses.

For each coating thickness investigated, 40–50 ELSP images were collected, aligned in both dimensions and then summed. The parallel recording of the position and energy axes in an ELSP image allows for the independent and accurate definition of the position of the coating. Our experimental setup allowed for the spatial sampling of the electronic properties of the coating with a resolution of ~3 Å. This was determined from a profile across the zero loss peak in the ELSP image, which is identical to the image of the coated nanotube integrated in the horizontal direction. Provided a suitable magnification is chosen, the ELSP profile (see Fig. 3) shows in this case WS₂ fringes which can be used for alignment and calibration of the spatial dimension in the ELSP images. Thus, we are able to sample the electronic structure of a linear feature on the nanoscale, using an instrument not ordinarily capable of forming probes smaller than 1.5 nm.

^{a)} Author to whom correspondence should be addressed; electronic mail: S.Silva@surrey.ac.uk

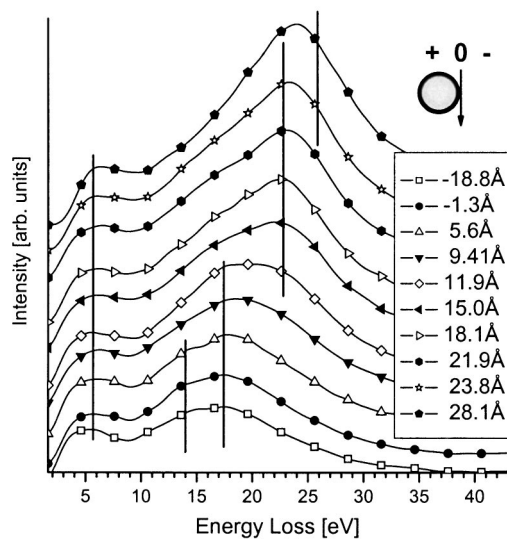


FIG. 1. Selected line spectra at various positions across the surface of a 4 ML WS_2 -coated MWCNT, after the removal of the zero-loss peak. The origin of the scale across the nanotube is defined at the outer surface of the coating, positive at positions inside the tube and negative outside (see inset diagram). The plasmon peak shows a transition from a dominant bulk mode to a surface plasmon dominant mode in the region of the coating. The dashed lines are guides to the eye for the positions of the various surface and bulk collective excitations in the region of the surface of the coating. The WS_2 coating fringes are clearly visible in the ELSP spatial dimension and can be used to determine the position of the coating independently.

Figure 1 shows low-loss spectra, after the removal of the zero-loss peak using a scaled-fitting method,⁹ at various positions from the outer surface of the 4-ML-coated nanotube, defined as negative outside the outer surface of the coating and positive towards the center of the MWCNT. When moving across the coated nanotube, the spectra in Fig. 1 show peaks at ~ 6 , ~ 18 , and ~ 23 eV, and also a further small peak at ~ 14 eV at grazing incidence and further from the coating (so-called “aloof” spectroscopy¹⁰).

The local anisotropy of the dielectric function and the hollow geometry of tubes result in a degeneracy of the surface plasmon mode into two or more modes.^{11–14} Previous work conducted on MWCNTs on the one hand^{11,12} and WS_2 nanotubes on the other^{13,14} have associated the bulk and surface plasmon peaks observed in Fig. 2 to a family of allowed interband transitions.¹² We use these individual studies as the starting point for the interpretation of our system combining the two cases. The peak at 23 eV is the bulk plasmon associated with the component of the dielectric function parallel to the local c -axis of the carbon tube (enhanced at the edge of the tube), while the bulk plasmon at 27 eV is associated with the perpendicular component of the dielectric function (enhanced in the middle of the tube).

The 17–18 eV peak is associated with the carbon tube’s surface plasmon of the σ electrons related to the σ - σ^* transition, the 14–15 eV peak is linked to π - σ^* and σ - π^* transitions, and the 6 eV peak represents surface excitations linked to the π - π^* transitions for the parallel component of the dielectric function.¹² The hollow geometry can further split these plasmon modes into symmetric and antisymmetric branches. For example,¹³ a thick pure WS_2 nanotube (ratio of inner to outer radii $r/R \ll 1$) shows, at grazing incidence, a dominant surface mode at ~ 16 eV which splits, for a thin nanotube ($r/R \sim 1$), into two modes centered on 15 and 22 eV. Similarly,¹¹ at grazing incidence, the 14–15 eV peak

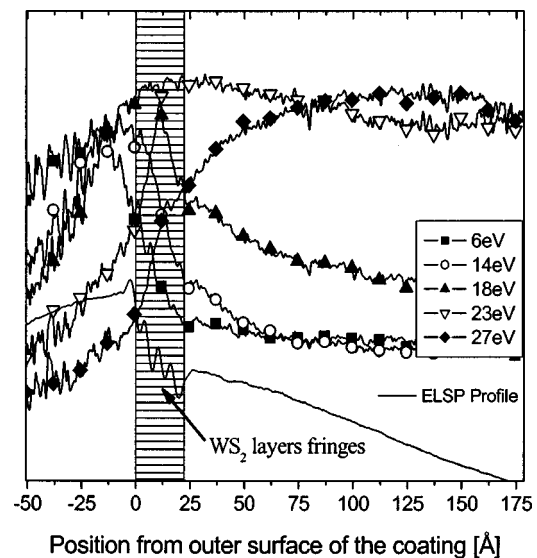


FIG. 2. Variation of areas of windows 2 eV wide and centered on 6, 14, 18, 23, and 27 eV as a function of position across MWCNTs coated with 4 ML of WS_2 . The area under the zero-loss peak is represented as the ELSP profile for each of the coating thicknesses and is used to determine accurately the position of the outer surface of the coating (i.e., the origin of the position scale), when compared to the image profile in each case. The hashed region marks the position of the coating layer, with negative positions being in the vacuum outside the nanotube.

for thick carbon tubes is shown to split into a radial mode at ~ 18 eV and a tangential mode at ~ 14 eV (Fig. 1).

As we step across the surface of the coated nanotube (Fig. 1), the relative weights of each of the peaks changes depending on the position from the outer surface of the coating. In our combined case, because of the overlap of the respective carbon and WS_2 surface and bulk peaks, we conclude that any interface plasmon between the tube and the coating will result in the modification the relative weights of the peaks in Fig. 1 according to the coating’s thickness. We investigate this relative change by normalizing each spectrum to the maximum value in the 4–35 eV range. Similar to the studies of Stephan *et al.*,¹¹ we used a 2 eV window centered on the dominant peaks to integrate the spectral intensity and display it as a function of position across the nanotubes.

Figure 2 shows typical measurements for the plasmon intensities from areas centered on 6, 14, 18, and 23 eV for a 4 ML coating. The ELSP profile shown is taken across the zero-loss peak in the ELSP images and is equivalent to the image of the nanotube integrated along that direction; it demonstrates the subnanometer spatial sampling and is used for the accurate determination of the scale and origin of the position axis. The origin of the position axis is determined in each case using the center of symmetry of the fringes from the ELSP profile, and then shifting the scale by half of the coating’s width where layers are separated by 6.2 Å and are ~ 3.2 Å thick.⁵ This shift effectively sets the origin of the spatial dimension on the outer surface of the coated nanotube, for easy comparison of MWCNTs with different WS_2 coating thicknesses. The hashed region in Fig. 2 is a visual representation of the coating’s width.

We repeated the experiment for several coating thicknesses, for all of which we observed a transition from the dominant bulk plasmon mode at 23 eV to the surface plasmon modes (18, 14, and 6 eV). We note that the position at which the transition between the bulk and surface plasmons

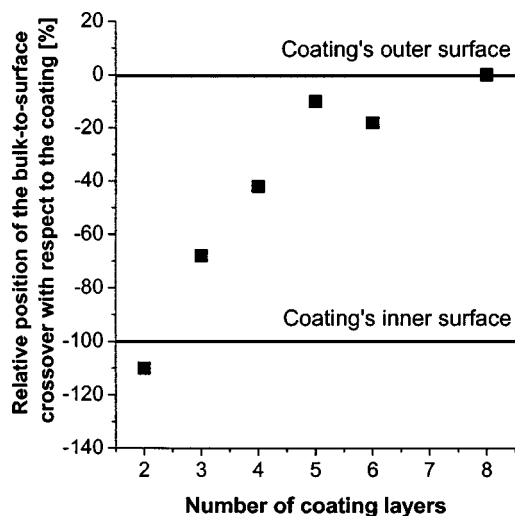


FIG. 3. The transition between the dominance of the bulk mode and that of the surface mode occurs at positions dependent on the coating thickness, displayed normalized to the coating's thickness: at the inner surface of the coating for 2 ML WS_2 , within the coating for 4 ML WS_2 , and at the outer surface of the coating for thicknesses above 5 ML of WS_2 . The error bars in the 2 ML case are $\sim 30\%$, but get smaller as the coating's thickness increases. In absolute terms, the error in position is $\sim 3 \text{ \AA}$.

(the crossover between the 18 and 23 eV curves) occurs with respect to the outer surface of the coating, depends on the thickness of the coating. Figure 3 summarizes the relative position of the crossover point with respect to the coating's surfaces, normalized to the width of the layer. For the 2 and 3 ML coatings, this transition occurs in the region of the inner surface of the coating, while for the 4 ML coating this occurs roughly in the middle of the coating. For coatings thicknesses beyond 5 ML, the transition occurs on the outer surface of the coating.

The variation in the bulk-surface changeover as a function of the position across the coated MWCNT can be interpreted in terms of the dielectric nature of the coating. One solution is that, when the coating is very thin, it acts as part of the surface of the MWCNT; for thicknesses equal or above 5 ML, the coating is thick enough to establish dielectric properties more akin to a pure WS_2 nanotube. In this model, the thin coatings (up to 4 ML) are seen to form a relatively dielectrically thicker outer surface of the MWCNT, with a less abrupt transition from vacuum to carbon nanotube. Once the thickness reaches 5 ML, there is now enough WS_2 for the coating to no longer be a dielectric part of the outer surface of the MWCNT so that there is now a sharp transition from the dielectric function of the MWCNT to that of the coating and then to that of the vacuum. However, because now we are in a situation similar to a pure WS_2 nanotube with a very small r/R radius, we expect^{13,14} to have a strong coupling of the surfaces leading to a split of the 16 eV surface mode into a peak at 22 eV and the "forest of peaks"¹³ at 0–15 eV. This peak in turn contributes to the signal in the 23 eV peak (Fig. 2) so that the bulk-to-surface transition now occurs on the outer surface of the coating.

An alternate hypothesis, still based on the dielectric definition of the inner and outer surfaces of the coating is that,

for the thin coating, the diffused outer surface of the MWCNT can also be represented by a "clean" MWCNT outer surface dielectric function, placed at a position within the diffused outer surface model. This could be used to explain the observed variation of the crossover position with changing coating thicknesses below 4 ML (Fig. 3). When the coating reaches 5 ML, then we revert to being able to define the two abrupt dielectric surfaces of the coating. In this case, the coupling between the coating and the MWCNT is now facilitated, such that the outer surface of the coating acts also as the outer surface of the MWCNT. This would interpret the observed crossover at the outer surface of the coating not as a contribution from a surface coupling of the interfaces of the coating, but simply as the outer surface of the coating being now dielectrically coupled with the MWCNT.

In conclusion, we have investigated experimentally the nature of the interface between a MWCNT and its WS_2 coating, as a function of the coating's thickness. This was achieved with subnanometer spatial resolution, using parallel illumination in a non-scanning TEM, by means of energy loss spectroscopic profiling. The minimum width of the WS_2 coating necessary for it to have defined dielectric internal and external interfaces, was found to be 5 ML.

We thank the EPSRC for funding through the Portfolio Grant and the Multidisciplinary project grant GR/N36073/01.

¹S. Iijima, *Nature (London)* **354**, 56 (1991).

²H. W. Kroto, J. R. Heath, S. C. O'Brien, R. F. Curl, and R. E. Smalley, *Nature (London)* **318**, 162 (1985).

³L. A. W. Robinson, S.-B. Lee, K. B. K. Teo, M. Chhowalla, G. A. J. Amaratunga, W. I. Milne, D. A. Williams, D. G. Hasko, and H. Ahmed, *Nanotechnology* **14**, 290 (2003).

⁴D. Cox, R. D. Forrest, P. R. Smith, and S. R. P. Silva, "Manipulation of Carbon Nanotubes for Construction of Bespoke Nano-Device Structures", in *Nanoengineered Nanofibrous Materials*, Proceedings of the NATO Advanced Study Institute, Belek-Antalia, Turkey, 1–12 September 2003, NATO Science Series II: Mathematics, Physics and Chemistry, <<http://www.springeronline.com/sgw/cda/frontpage/0,11855,3-185-69-33107180-0,00.html>>, Vol. 169, Guceri, Selcuk; Gogotsi, Yury G.; Kuznetsov, Vladimir (Eds.) 2004, XII, 543 p., Softcover. ISBN: 1-4020-2549-1; pg. 311-xxx.

⁵R. L. D. Whitby, W. K. Hsu, P. K. Fearon, N. C. Billingham, I. Maurin, H. W. Kroto, D. R. M. Walton, C. B. Boothroyd, S. Firth, R. J. H. Clark, and D. Collison, *Chem. Mater.* **14**, 2209 (2002); R. L. D. Whitby, W. K. Hsu, C. B. Boothroyd, H. W. Kroto, and D. R. M. Walton, *Chem. Phys. Lett.* **359**, 121 (2002).

⁶L. Reimer, I. Fromm, P. Hirsch, U. Plate, and R. Rennekamp, *Ultramicroscopy* **46**, 335 (1992).

⁷T. Walther, *Ultramicroscopy* **96**, 401 (2003).

⁸*Philips Operating Instructions CM200TEM*, 1st ed. (rev.), Philips Electronics N.V. (Eindhoven, Netherlands, 1994/1995) p. 2–24.

⁹B. W. Reed and M. Sarikaya, *Ultramicroscopy* **93**, 25 (2002).

¹⁰R. J. Warmack, R. S. Becker, V. E. Anderson, R. H. Ritchie, Y. T. Chu, J. Little, and T. L. Ferrell, *Phys. Rev. B* **29**, 4375 (1984).

¹¹O. Stéphan, M. Kociak, L. Henrard, K. Suenaga, A. Gloter, M. Tencé, E. Sandré, and C. Colliex, *J. Electron Spectrosc. Relat. Phenom.* **114–116**, 209 (2001); *Phys. Rev. B* **66**, 155422 (2002).

¹²M. Kociak, L. Henrard, O. Stéphan, K. Suenaga, and C. Colliex, *Phys. Rev. B* **61**, 13936 (2000).

¹³M. Kociak, O. Stéphan, L. Henrard, V. Charbois, A. Rothschild, R. Tenne, and C. Colliex, *Phys. Rev. Lett.* **87**, 075501 (2001).

¹⁴D. Taverna, M. Kociak, V. Charbois, and L. Henrard, *Phys. Rev. B* **66**, 235419 (2002).